

# Experimental and Theoretical Studies of Seismoelectric Effects in Boreholes

Zhenya Zhu, Shihong Chi, and M. Nafi Toksöz

Earth Resources Laboratory  
Dept. of Earth, Atmospheric and Planetary Sciences  
Massachusetts Institute of Technology  
Cambridge, MA 02142

## Abstract

In a fluid-saturated porous formation, an impinging seismic wave induces fluid motion. The motion of fluid relative to the rock frame generates an electric streaming current. This current produces electric and magnetic fields, which are called seismoelectric and seismomagnetic fields, respectively. When there is a fracture or a discontinuity, a radiating electromagnetic wave is also generated, in addition to local fields. Seismoelectric and seismomagnetic fields depend on the amplitude, frequency, and mode of the seismic wave, as well as the formation porosity, permeability, pore size, and fluid conductivity. In this paper, we describe laboratory results of seismoelectric and seismomagnetic fields induced by an acoustic source in borehole models. We use a piezoelectric source for acoustic waves and a point electrode and a high-sensitivity Hall-effect transducer for measuring the localized seismoelectric and seismomagnetic fields in fluid-saturated rocks. The dependence of seismoelectric conversions on porosity, permeability and fluid conductivity are investigated. Three components of the seismomagnetic field are measured by the Hall-effect transducer. At a horizontal fracture, the acoustic wave induces a radiating electromagnetic wave.

Further, we conduct theoretical and numerical studies of electrokinetic conversions in fluid-filled boreholes. First, we derive the mathematical formulations for seismoelectric responses for an acoustic source in a borehole. Then we compute the electric field in boreholes penetrating formations with different rock compressibility, permeability, and porosity. We analyze the sensitivity of the converted electric fields to formation permeability and porosity. We find that the ratio of magnitude of electromagnetic waves to that of acoustic pressure increases with increasing porosity and permeability in fast and slow formations. Seismoelectric and seismomagnetic well logging might be a new means to determine formation properties in a borehole.

## INTRODUCTION

When a porous rock is saturated with water, an electric double layer (EDL) is formed at the boundary between solid and fluid. An acoustic wave propagating in the material induces fluid motion, which generates an electric current. This current produces electric and magnetic fields, which are called seismoelectric and seismomagnetic fields, respectively. Theoretical studies (Haartsen, 1995, Pride and Haartsen, 1996) confirm the mechanism of the conversion. Inside a homogeneous, porous medium, the seismic wave induces localized seismoelectric and

seismomagnetic fields. At an interface, the acoustic wave induces a radiating electromagnetic (EM) wave. Laboratory experiments (Morgan et al., 1989, Zhu et al., 2000) measured the seismoelectric fields induced by acoustic waves in scaled models. Field experiments (Thompson and Gist, 1993, Butler et al., 1996) measured seismoelectric signals on the ground. Seismoelectric borehole logging (Mikhailov et al., 2000, Hunt, C. W., and Worthington, 2000) indicates a strong relationship between a seismoelectric response and a fracture. Hu et al (2000, 2002) simulated the electric waveforms using the Pride equations. Markov and Verzhbitskiy (2004) simulated EM fields induced by acoustic multipole source in a borehole. In this paper, we model the EM fields due to acoustic sources in a borehole, and analyze the sensitivities of the electric signals to formation properties.

In a saturated porous rock or a fluid-saturated fracture where a fluid electrolyte comes into contact with a solid surface, anions from the electrolyte are chemically adsorbed to the solid rock leaving behind a net excess of cations distributed near the wall (Reppert and Morgan, 2002). This region is known as the EDL. A seismic wave propagating in the formation induces fluid motion and the fluid motion relative to the rock frame generates an electric streaming current. This current produces electric and magnetic fields, which are called seismoelectric and seismomagnetic fields, respectively. The fields induced inside a homogeneous medium is a localized field, which exists only in the area disturbed by the acoustic wave. At an interface between media with different properties (such as porosity, permeability, conductivity, or lithology), the acoustic wave induces a radiating electromagnetic wave, which propagates with EM wave speed and can be received anywhere.

Seismoelectric conversion depends on the electrolyte conductivity when the conductivity is low. When the EDL is saturated, the electric field amplitude decreases when the conductivity increases. Because the seismomagnetic field only depends on the movable charges in the fluid, the seismomagnetic amplitude increases when the conductivity increases. The seismomagnetic field is a vector field, we may measure its three components with different positions of the Hall-effect sensor. We also conduct theoretical and numerical modeling of seismoelectric conversion in a borehole for monopole and dipole logging.

We first demonstrate the seismoelectric phenomena with a set of laboratory experiments. The particular geometry we use is related to borehole measurements (e. g. acoustic/electric logging) in the earth. Laboratory models are scaled down using the acoustic wavelength scaling. Borehole models are made to simulate a layered earth, and boreholes with horizontal and/or vertical fractures. An acoustic transducer, an electrode, and a Hall-effect sensor are applied to record the acoustic wave, electric and magnetic fields induced by an acoustic wave.

## **LABORATORY EXPERIMENTS**

To study the seismoelectric effects in the laboratory, three physical borehole models, a layered borehole, a borehole with horizontal fracture, and a borehole with horizontal/vertical fractures, were made with natural rocks and Lucite. The layered borehole model was made of two materials (slate and Lucite) with a horizontal interface, but without a fracture between the layers. The second borehole model was made of Lucite and slate blocks with a horizontal fracture of 0.5 mm aperture. The third model has the same horizontal fracture and a vertical fracture across the borehole in the Lucite section. The diameter of the boreholes is about 10 mm.

The acoustic source is a cylindrical PZT transducer of 9 mm in diameter. A square pulse of 750 V amplitude and 10  $\mu$ s width excites the source. Three kinds of receivers (acoustic transducer, point electrode, and Hall-effect device) were used to record the acoustic, electric, and magnetic fields in the borehole. The Hall-effect device used in our experiments is a magnetic sensor whose output is proportional to the magnetic flux density and the direction of the magnetic field. This device does not respond to the magnetic component of any electromagnetic wave. The models are placed in a tank with water of 65  $\mu$ S/cm conductivity.

When the acoustic source is fixed in boreholes, receivers move gradually in the borehole and record the acoustic, electric, and magnetic signals in the three borehole models.

In a layered slate-sandstone borehole, we recorded the acoustic and electric signals generated by a monopole acoustic source. Figure 1 shows the borehole model (a), recorded acoustic (b) and electric(c) signals, and (d) electric amplitude normalized by the acoustic amplitude, the propagation velocities of the acoustic wave and the electric signals are the same, confirming that the acoustic wave induces the localized electric field. The amplitudes of the electric signals are directly proportional to the acoustic amplitude. The electric to acoustic ratio depends on the porosity, permeability, and conductivity in a given rock. This is demonstrated in Fig. 1(d).

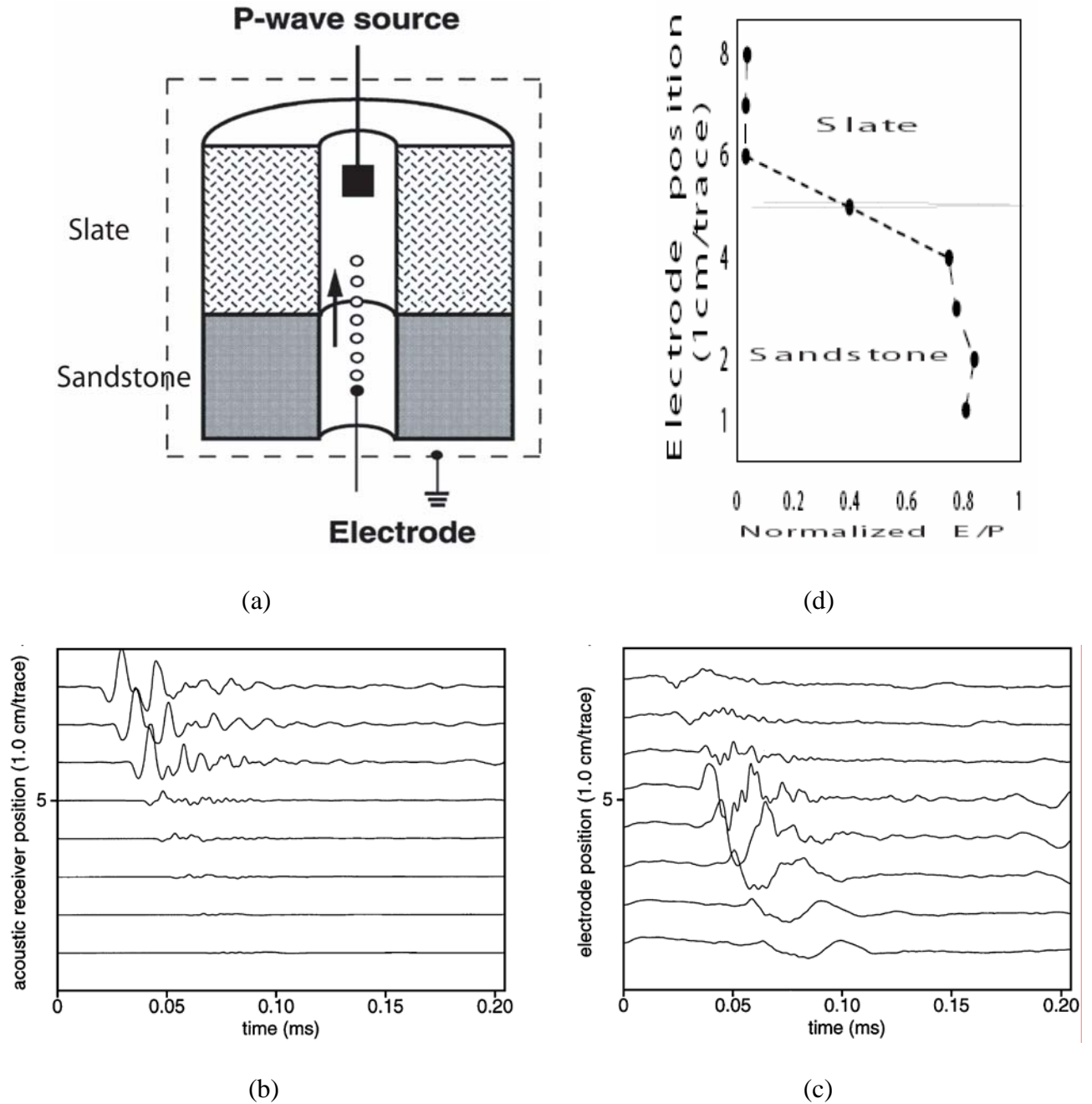


**FIGURE 1.** A borehole model (a) with slate and sandstone layers, acoustic waveforms (b), electric signals (c), and (d) electric amplitude normalized by acoustic amplitude in the borehole.

Figure 2 shows the borehole model (a) with a horizontal fracture, recorded acoustic (b), electric (c), and magnetic (d) signals. The Stoneley wave in the slate section (traces 1-5 in Fig. 1c) induces electric signals, whose apparent velocity is the same as the Stoneley wave.

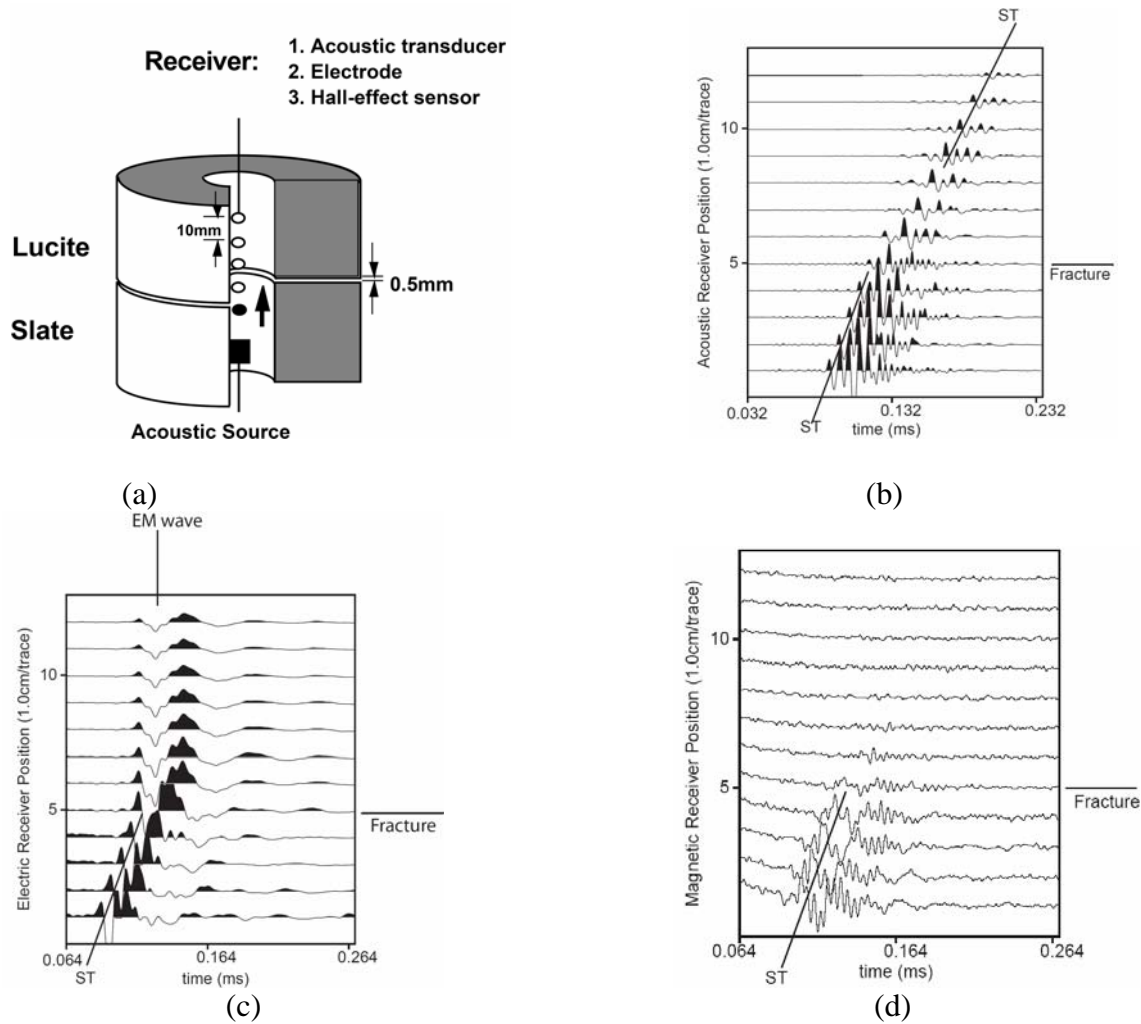


**FIGURE 2.** A borehole model (a) with a horizontal fracture between slate and Lucite, acoustic waveforms (b), electric signals (c), and magnetic signals (d) received in the borehole. Lines “ST” indicate the propagation of the Stoneley waves.

At the fracture, the Stoneley wave induces an EM wave, whose velocity is that of an electromagnetic wave in the borehole (traces 6-12 in Fig. 1c). The Hall-effect device records the horizontal component of the magnetic field induced by the Stoneley wave in the slate section. The Hall-effect device does not record the magnetic component of an electromagnetic wave, as shown in Fig. 2(d)

The results confirm that acoustic waves induce stationary or localized electric and magnetic fields in a porous formation, and induce a radiating electromagnetic wave at a horizontal fracture due to its discontinuity. Additional measurements have been made in models that contain both horizontal and vertical fractures.

## THEORETICAL AND NUMERICAL STUDIES

Beyond the experimental studies, we also conduct theoretical and numerical studies of electrokinetic conversions in fluid-filled boreholes.

## Mathematical Formulation Of The Multipole Seismoelectric Field

Using to Pride's equations (1994) for seismoelectric wave propagation in porous media, the electric current density  $\bar{J}$  can be written as

$$\bar{J} = \sigma \bar{E} + L(-\nabla p + \omega^2 \rho_f \bar{u}), \quad (1)$$

and the displacement of the fluid phase  $\bar{w}$  can be expressed as

$$-i\omega \bar{w} = L\bar{E} + \frac{k}{\eta}(-\nabla p + \omega^2 \rho_f \bar{u}), \quad (2)$$

where  $\bar{u}$  is the displacement of the solid frame,  $p$  is the pore pressure,  $\bar{E}$  is the electric field strength,  $L$  is the coupling coefficient,  $\rho_f$  and  $\eta$  are the density and the viscosity of the pore fluid, respectively,  $k$  and  $\sigma$  are the dynamic permeability and conductivity of the porous medium, and  $\omega$  is the angular frequency.

Hu and Liu (2002) introduced two assumptions to approximate the seismoelectric wave fields. They first showed that the converted electric field affects the elastic field negligibly and the coupling term in equation (2) can be ignored. They also assumed that the electric field is time invariant within the acoustic logging operation framework, because the EM wavelength is much longer than the tool length. Under this quasi-static condition, the electric field can be written as the gradient of an electric potential

$$\bar{E} = -\nabla \phi. \quad (3)$$

They showed that the electric potential and the potential of the gradient field of the solid displacement are related as follows:

$$\nabla^2 \phi = \frac{L}{\sigma}(-\nabla^2 p + \omega^2 \rho_f \nabla^2 \varphi). \quad (4)$$

In wave number domain, the solution to Equation (4) is

$$\phi_n = A_{em} K_n(k_{em} r) \cos n\theta + \frac{L}{\sigma}(-p + \omega^2 \rho_f \varphi), \quad (5)$$

where  $A_{em}$  is an unknown coefficient,  $k_{em}$  is the axial wavenumber of the EM wave. The pore pressure can be written as:

$$p = \sum_{j=1}^2 [(Q + \tilde{R} \xi_j) l_j^2 / \phi_0] A_j I_n(k_{pf} r_0) K_n(k_{pj} r) \cos n\theta, \quad (6)$$

where  $Q$ ,  $\tilde{R}$ , and  $\xi_j$  are defined by Biot (1956a), wavenumber  $l_j^2 = \frac{\omega^2}{\alpha_j^2}$ ,  $\phi_0$  is formation porosity, and  $A_j$  is a unknown coefficient, and  $r_0$  is the radius of the circle of monopole point source distribution.

The potential function  $\varphi_j$  can be written as

$$\varphi_j = A_j I_n(k_{pf} r_0) K_n(k_{pj} r) \cos n\theta. \quad (7)$$

The potential function  $\varphi_j$  is a solution for a multipole source of order  $2n$ . Index  $j$  indicates fast and slow wave in porous media.

We obtain the electric field using equation (3). In formation,

$$E_z = -ik_{em} \phi_n, \quad (8)$$

and  $J_r$  can be derived from equation (1).

In borehole fluid, we assume the electric potential to be

$$\phi_f = -ik_{em} B_{em} I_n(k_{em} r) I_n(k_{pj} r_0) \cos n\theta \quad (9)$$

where coefficient  $B_{em}$  is to be determined. The electric current density in borehole can also be derived from equation (1).

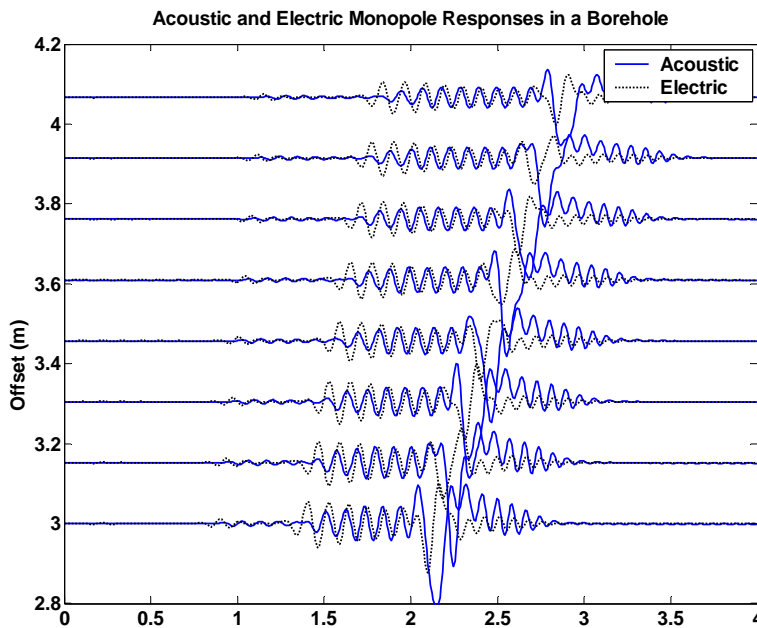
### Boundary Conditions At The Borehole Wall

Across the borehole wall, the tangential electric field and normal magnetic field are continuous. This boundary condition is equivalent to the electric potential and radial current continuity. Then we obtain a set of linear equations and can solve for unknown coefficients  $A_{em}$  and  $B_{em}$ . Finally, we can compute the electric fields in formation and borehole fluid.

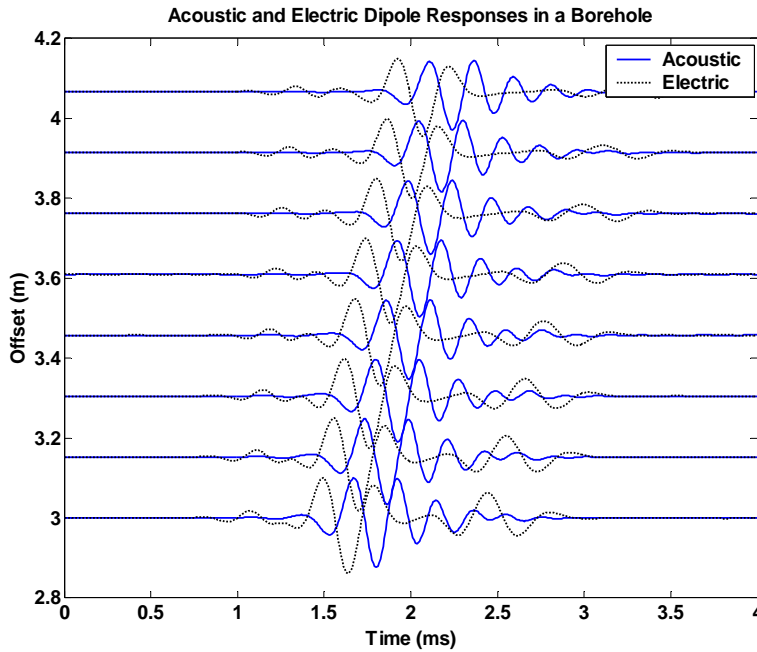
### Numerical Computation of The Multipole Seismoelectric Field

We compute the electric field in boreholes formations with high and low rock compressibility, permeability, and porosity. Figure 3 compares the monopole and dipole wave fields for a fast formation. Figure 3(a) shows that P, pseudo-Rayleigh, and Stoneley wave modes all generate local EM waves, but the Stoneley mode has the highest amplitude in acoustic and EM wave fields.

We study the sensitivity of the seismoelectric conversion to formation porosity and permeability in dipole logging. Figure 4 shows the EM wave conversion rate for the high permeability (1 darcy) rock is about 25 times higher than that for the low permeability (1 mili-darcy) rock. When we study the sensitivity to porosity, we fix the permeability to 100 mili-darcy and vary the porosity from 5% to 30%. Figure 5(a) shows that the conversion ratio is not very sensitive to porosity. Then we fix the porosity to 20% and vary the permeability from 1 mili-darcy to 1 darcy. Figure 5 (b) shows that the acoustic to electric conversion rate increases almost linearly with the logarithm of permeability.



(a)



(b)

**FIGURE 3.** Comparison of (a) monopole and (b) dipole responses in borehole. For each source, the acoustic and electric signals are plotted on top of each other. They are 90 degree out of phase.

## CONCLUSIONS

An electric double layer at the interface between rock and water induces electric and magnetic fields when an acoustic wave propagates in the system. The acoustic wave in a homogeneous borehole induces localized seismoelectric and seismomagnetic fields. At a horizontal fracture, the acoustic wave induces a radiating electromagnetic wave due to the discontinuity of the borehole.

Seismoelectric conversion depends on the formation properties, such as porosity, permeability, lithology, and fluid conductivity and mobility.

Acoustic, electric and magnetic fields provide properties of the porous formation. We find that seismoelectric conversion rate is very sensitive to permeability in formations with high and low seismic velocities. Therefore, the seismoelectric and seismomagnetic measurements may be a new logging technique for formation evaluation.

## ACKNOWLEDGMENTS

This work was supported by the Borehole and Acoustic Logging Consortium and the Founding Members of the Earth Resources Laboratory at Massachusetts Institute of Technology.

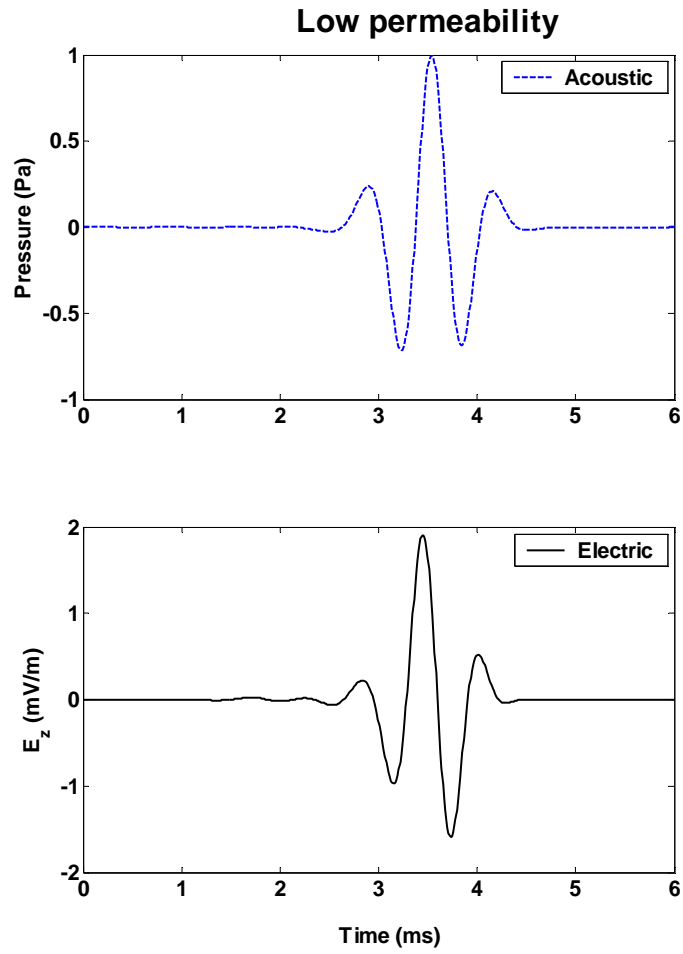
## REFERENCES

1. Biot, M. A., 1956a, Theory of propagation of elastic waves in a fluid saturated porous rock. I. low frequency range: *J. Acoust. Soc. Am.*, 28, 179-191.
2. Butler, K. E., Russell, R., Kepic, A., and Maxwell, M., 1996, Measurement of the seismoelectric response from a shallow boundary: *Geophysics*, 61, 1769-1778.
3. Haartsen, M. W., 1995, Coupled electromagnetic and acoustic wavefield modeling in poro-elastic media and its application in geophysical exploration. Ph. D. Thesis, Massachusetts Institute of Technology.
4. Hu, H., and Liu, J., 2002, Simulation of converted electric field during acoustoelectric logging: SEG Intl. Exposition and 72<sup>nd</sup> Annual Meeting.
5. Hu, H., Wang, K., and Wang, J., 2000, Simulation of acoustically induced electromagnetic field in a borehole embedded in a porous formation: Borehole Acoustic and Logging and Reservoir Delineation Consortia Annual Report, Earth Resources Laboratory, MIT.
6. Hunt, C. W., and Worthington, M. H., 2000, Borehole electrokinetic responses in fracture dominated hydraulically conductive zones: *Geophysical Research Letters*, 27, 9, 1315-1318.
7. Markov, M. G., 2004, Simulation of the electroseismic effect produced by an acoustic multipole source in a fluid-filled borehole: SPWLA 45<sup>th</sup> Annual Logging Symposium.
8. Mikhailov, O. V., Queen, J., and Toksöz, M. N., 2000, Using borehole electroseismic measurements to detect and characterize fractured (permeable) zone: *Geophysics*, 65, 1098-1112.
9. Morgan, F. D., Williams, E. R., and Madden, T. R., 1989, Streaming potential properties of westerly granite with applications: *Journal of Geophysical Research*, 94, 12449-12461.
10. Pride, S. R. and Haartsen, M. W., 1996, Electroseismic wave properties: *J. Acoust. Soc. Am.*, 100, 1301-1315.
11. Pride, S. R., 1994, Governing equations for the coupled electromagnetics and acoustics of porous media: *Physical Review*, B, 50, 15678– 15696.
12. Pride, S. R., and Morgan, F., 1991, Electrokinetic dissipation induced by seismic waves: *Geophysics*, 56, 914-925.
13. Reppert, P. and Morgan, F. D., 2002, Frequency-dependent electroosmosis: *Journal of Colloid and interface Science*, 254, 372-383.
14. Thompson, A. H. and Gist, G. A., 1993, Geophysical applications of electrokinetic conversion: *The Leading Edge*, 12, 1169-1173.
15. Zhu, Z. and Toksöz, M. N., 2002, Crosshole seismoelectric measurements in borehole models with fractures, 72th SEG Annual International Meeting Expanded Abstracts, BH2.2, 344-347.
16. Zhu, Z., Haartsen, M. W., and Toksöz, M. N., 2000, Experimental studies of seismoelectric conversions in fluid-saturated porous media: *Journal of Geophysical Research*, 105, 28,055-28,064.

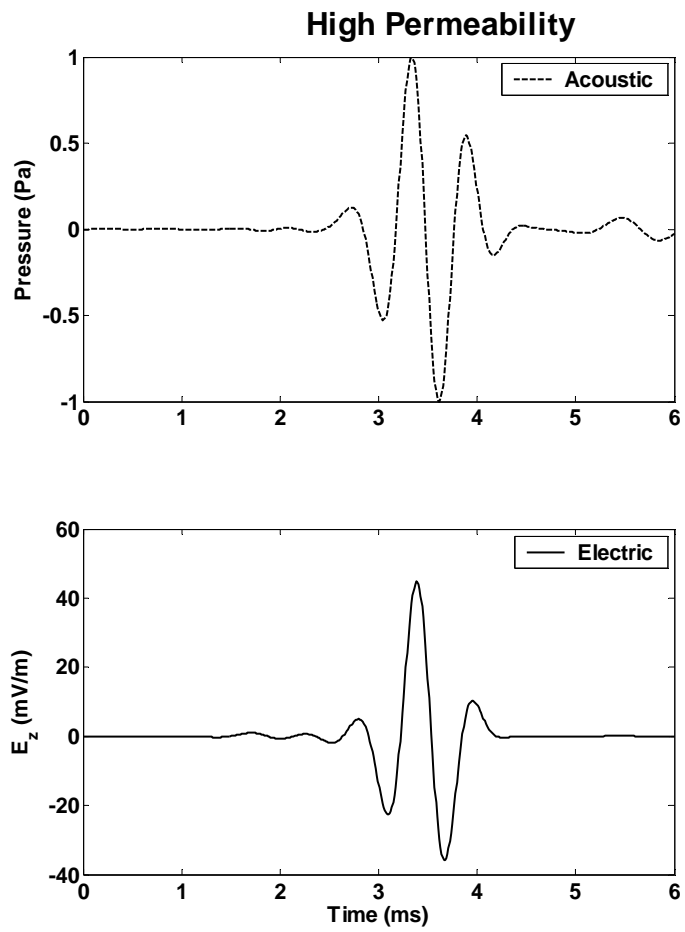


	Porosity (%)	Ks (GPa)	Solid density (kg/m <sup>3</sup> )	Solid Vp (m/s)	Solid Vs (m/s)
Slow formation	20	35	2600	2000	1200

**TABLE 1.** The slow formation parameters

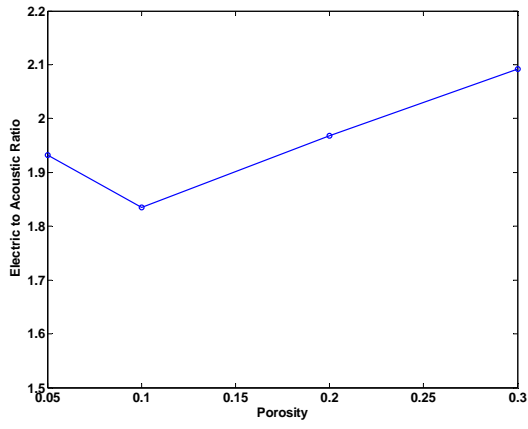


(a)

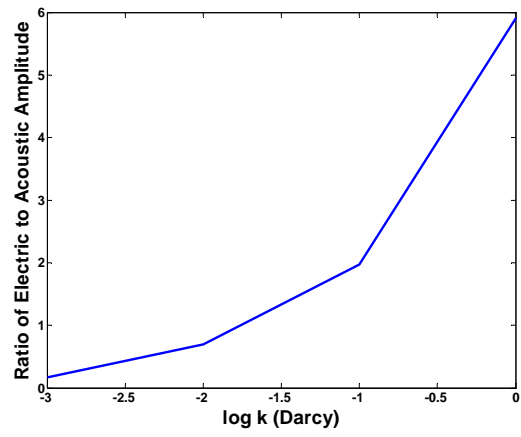


(b)

**FIGURE 4.** Comparison of dipole responses in (a) low (1.0md) and (b) high (1.0d) permeability rocks. Note we use the different scales for the electric fields. Table 1. shows the slow formation parameters.



(a)



(b)

**FIGURE 5.** Sensitivity of the ratio of electric to acoustic amplitude to (a) porosity and (b) permeability in the slow formation.